GIA NEWS FROM RESEARCH

Separation of Natural Red Andesine from Tibet and Copper-Diffused Red Andesine from China

Ahmadjan Abduriyim and Ross Pogson

Abstract

The question of a natural red andesine occurrence in Tibet has been the source of great controversy since 2006. In an attempt to put this matter to rest, an international group conducted field research on Tibetan andesine in October 2008 and in late September 2010. The alleged deposits are located at the village of Zha Lin and in the Yu Lin Gu Valley in Bai Nang County, ~3 km from the previously investigated Nai Sa village–Bai Nang mining area and about 55 km of southeast of Shigatse. Meanwhile, commercial treatment by diffusing copper into andesine was reportedly ongoing in China. The starting material for this process was said to be pale yellow andesine from Gu Yang County, Inner Mongolia, China. This article presents additional details on the morphological appearance and the geochemical and powder X-ray diffraction properties of these Tibetan samples as well as Cu-diffused samples from Xi'an and Shen Zhen in China. Some of the natural-color Tibetan samples proved indistinguishable from Cu-diffused Inner Mongolian andesine using laboratory techniques, although destructive analytical methods may establish feasible identification criteria.

INTRODUCTION AND BACKGROUND

To address whether natural red plagioclase feldspar-andesine occurs in Tibet, the author and five gem dealers and a gemologist visited an alleged deposit called Bainang (or Bai Lang) in 2008. The deposit is located near the village of Nai Sa, ~55 km southeast of Shigatse (or Xigazê; see figure 1; Abduriyim, 2008, 2009a,b). Copper-bearing red andesine of gem quality has been found in the mine, which is owned by Li Tong of China. The internal features and chemical composition of the Tibetan samples collected on the 2008 expedition closely resembled the allegedly copper-diffused Inner Mongolian red andesine available on the market, to the degree that doubt was cast on the natural origin of the Tibetan stones (Hughes, 2010; Rossman, 2011).

In an effort to resolve the controversy, another field trip to Tibet was carried out in late September 2010. They studied the reported Tibetan andesine occurrences at Zha Lin village and Yu Lin Gu (Abduriyim and Laurs, 2010; Abduriyim et al., 2010; Hughes, 2010; Leelawatanasuk, 2010). These areas are located ~3 km from the Nai Sa–Bainang mining area, which the author visited in 2008. Due to the objection of a local monk who controls access to the land in this area, the party was unable to visit the Bainang mine. The villagers interviewed by the expedition said the orange-red stones have been known in this part of Tibet for several decades or longer.

A brief excerpt of the research on andesine from three localities in Tibet and the known Cu-diffusion treated andesine

from Xi'an and Shen Zhen was published in the summer 2011 issue of *Gems & Gemology*. The geologic field information gathered by the expedition group was also included in that comprehensive article.

This article introduces more detailed photos and figures laboratory testing of the samples the author collected, including surface features, chemical and gemological properties, and structural order as revealed by power X-ray diffraction.

Figure 1. The reported andesine mines visited by Abduriyim's 2008 and 2010 expedition are located in south-central Tibet, ~55 km from Shigatse.

MATERIALS AND METHODS

All samples described in this article were obtained during the author's 2008 and 2010 expeditions. These were personally collected by expedition members (for samples from Zha Lin and Yu Lin Gu, see figure 2a,b) and collected near the Nai Sa village. The Bainang mine area (see figure 2c). In Guangzhou, the group obtained two additional lots of red andesine that were reportedly copper-diffused in China using Inner Mongolian pale yellow andesine as the starting material. These were treated either in Xi'an in 2004–2005 or in Shenzhen in 2007–2008 (figure 3a,b).

Standard gemological properties (RI, SG, UV fluorescence, Chelsea filter reaction, spectroscopic observations, and microscopic characteristics) were obtained for 198 pieces of reddish orange to orange-red andesine from Zha Lin and Yu Lin Gu. Of these, 95 were polished with two parallel windows and cleaned with acetone and aqua regia in an ultrasonic bath to remove surface contamination. In addition, 50 known-treated red andesines (from Xi'an and Shenzhen) were characterized.

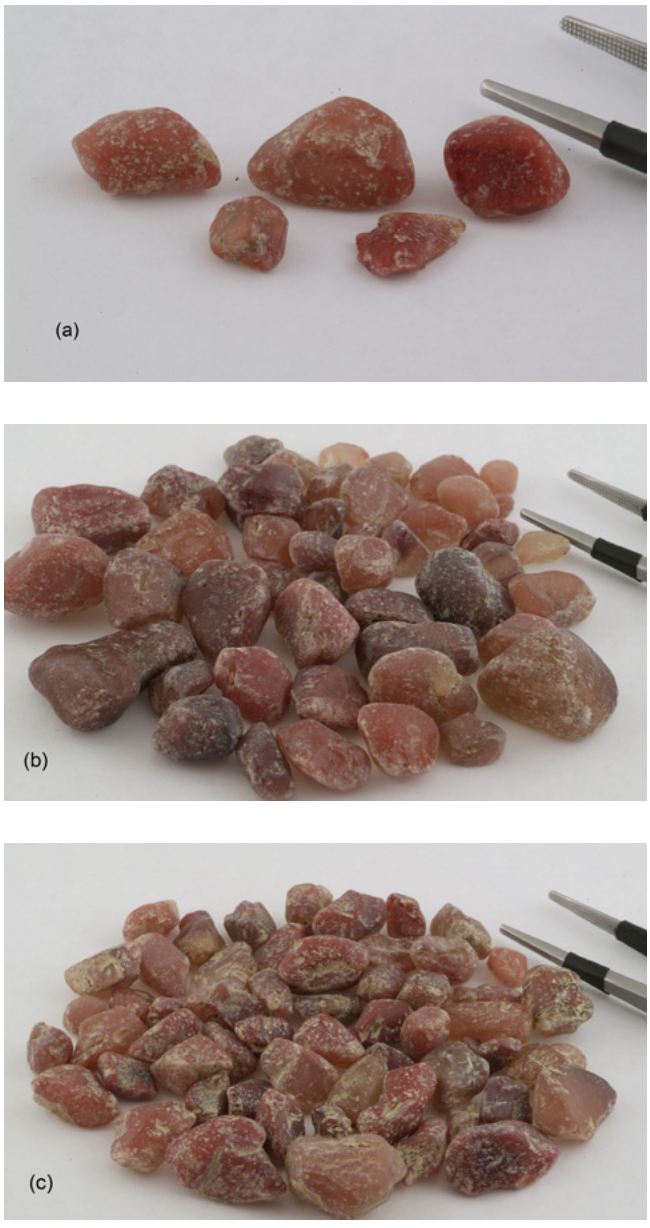

Figure 2. A pile of andesine rough samples obtained by Abduriyim's 2008 and 2010 expedition are shown here. (a) The samples are from Zha Lin (0.12–1.09 g), (b) Yu Lin Gu (0.20–3.20 g), and (c) Nai Sa–Bainang (0.11–2.92 g). Photo by A. Abduriyim.

Figure 3. These red andesine samples, offered by Litto Gems Ltd, were reportedly treated in China using the Inner Mongolian starting material. The samples in (a) were said to have been treated in Xi'an in 2004–2005, and those in (b) were reportedly treated in Shenzhen in 2007–2008. Photo by A. Abduriyim.

Quantitative chemical analysis using a JEOL JXA-8500 electron microprobe was carried out at NIMS (Tsukuba, Japan) on the polished surfaces of eight orange-red and red samples (two each, obtained from Zha Lin and Yu Lin Gu during the 2010 expedition, and two each of the known-treated stones from Xi'an and Shen Zhen). Five spots were analyzed on each sample. The operating conditions included an accelerating voltage of 15 kV, a beam current of 7 nA, and count times of 20 seconds on peaks and 5 seconds on backgrounds.

LA-ICP-MS trace-element data were obtained for 80 orange-red to red Tibetan samples (20 from Zha Lin and 40 from Yu Lin Gu obtained in 2010, and 20 from the author's 2008 expedition to Nai Sa–Bainang); 45 known-treated red samples (22 from Xi'an and 23 from Shenzhen); and 12 pale yellow pieces from Inner Mongolia. The instrumentation consisted of a New Wave Research UP266 laser ablation system coupled to an Agilent 7500a series ICP-MS at the GEMOC Key Centre at Macquarie University in Sydney, Australia. Operating conditions were 5 Hz repetition rate, 60 μm spot diameter, 120 second laser dwell time, and 80% laser power output (4.5 J/cm^2). Three spots were ablated per sample. NIST 610 glass was the primary external calibration standard, and BCR basalt was the secondary standard to correct mass bias. Aluminum was the internal standard element, based on an average Al_2O_3 concentration of 28% determined by microprobe analysis. The data were processed with the Glitter software package (Van Achterbergh et al., 1999) developed by GEMOC and CSIRO Exploration and Mining. To evaluate the usefulness of trace-element data in separating andesine from various sources, a multivariate statistical method (developed by Agilent) was used to examine relationships among multiple isotopes simultaneously. Ten isotopes (^{39}K, ^{49}Ti, ^{57}Fe, ^{69}Ga, ^{88}Sr, ^{107}Ag, ^{137}Ba, ^{139}La, ^{140}Ce, and ^{208}Pb) were categorized into two parameters as component 1 and component 3, and data were plotted into a principal component diagram.

Powder X-ray diffraction measurements of 42 samples were taken at the Australian Museum to investigate whether the feldspar's lattice (unit cell) parameters were indicative of treatment. These consisted of 20 pieces of orange-red and red andesine from Tibet (5 from Zha Lin, 5 from Yu Lin Gu, and 10 from Nai Sa–Bainang); 10 red known-treated stones (five each from Xi'an and Shenzhen); and 12 pale yellow samples from Inner Mongolia. Data were collected with a Shimatsu LabX XRD-6000 X-ray diffractometer, using CuKα radiation (λ = 1.5406 Å) with beam conditions of 40 kV and 30 mA. Diffraction data were collected over a range of 7–70° 2θ with a step interval of 0.02° 2θ and a count time of 1 second/step. The lattice parameters were calculated by the least-squares method using CELLCalc software, with the well-known parameter of $\Delta 2\theta = 2\theta_{1\bar{3}1} - 2\theta_{131}$ to determine structural states based on the spacing between the $(1\bar{3}1)$ and (131) peaks of the powder X-ray diffraction pattern (Ribbe, 1972). To test whether the Δ2θ parameters were changed by heating, two pale yellow Inner Mongolian samples were selected for copper diffusion experiments. Each sample was cut into

two pieces. Half of one sample (INMG-DF-001a) was buried in ZrO_2 powder mixed with 2–3% copper powder and diffused at 1160°C for 50 hours; half of the other stone (INMG-DF-002a) was packed into Al_2O_3 powder mixed with 2–3% copper powder and heated at 1050°C for 24 hours. The remaining halves were retained as control samples.

RESULTS AND DISCUSSION

Gemological Observations

The andesine samples collected from Zha Lin and Yu Lin Gu were generally indistinguishable from one another and from those obtained in Nai Sa village. All of the andesines from these localities were rounded. Most of the stones were transparent to translucent, and their overall gemstone quality was not high (again, see figure 2). In fact, very few of the samples would be expected to yield high-quality cut gemstones. Most of the pieces were under a centimeter, and the largest reached ~2 cm. Their color was mostly pale orangy red or red, though a rare few had a pure red color. Compared to andesine from the Nai Sa–Bainang area, the Zha Lin and Yu Lin Gu samples generally were a weaker red. Some showed green or bluish green zones or patches; any surface-reaching fractures were surrounded by a narrow colorless zone (see figure 4). In addition, a few of the Yu Lin Gu samples showed a distinct yellow color zone near the surface. Most also had a narrow colorless rim along the surface, and some stones showed concentric color zoning with green-blue and red bands.

None of the Tibetan samples exhibited a good crystal form. They had a smooth water-worn appearance and generally round, elongated faces. A few had broken cleavage surfaces. Some of the andesines also featured embayed areas that appeared to have been created by chemical etching, while some areas displayed a melted glassy surface (figure 5a and b).

The samples' refractive index and specific gravity fell in the range for the andesine variety of plagioclase feldspar. They gave a weak chalky orange reaction to long-wave UV radiation, and dark red or inert under short-wave UV. Under a Chelsea color filter, the andesine remained red. Some red stones appeared green in diffused transmitted light, and a

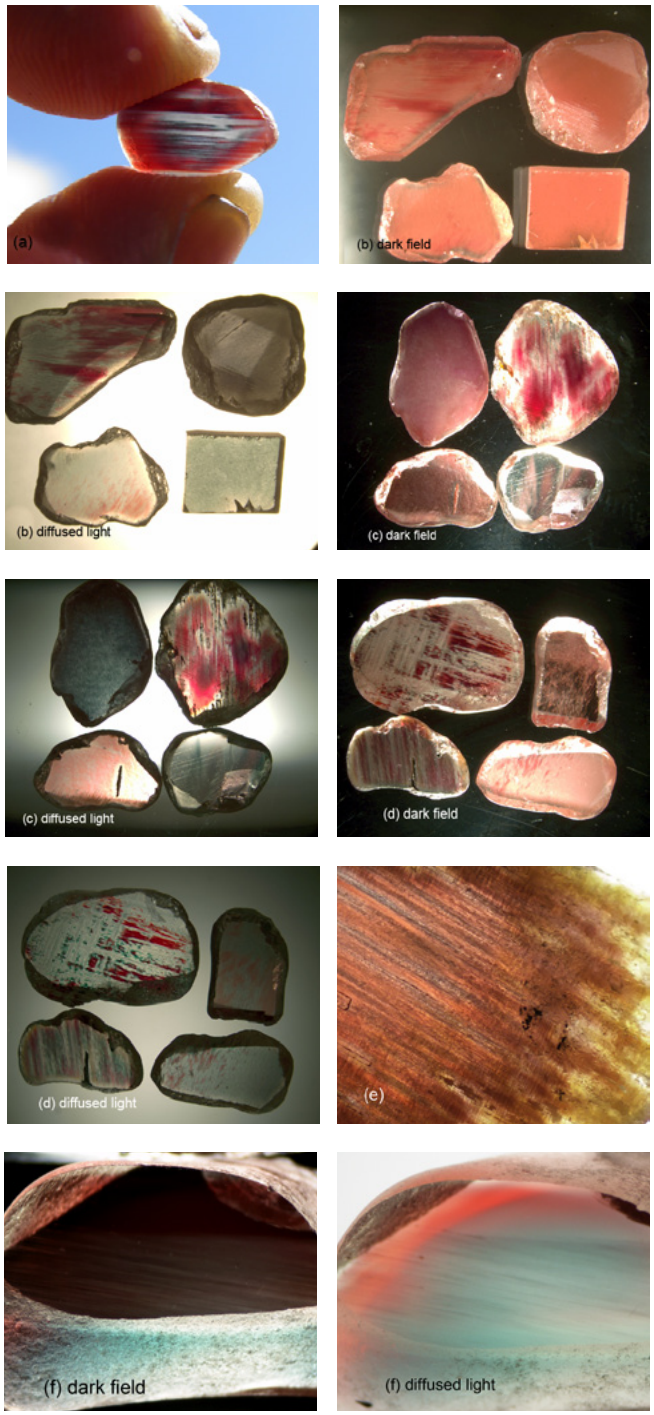

Figure 4. These Tibetan andesine samples (0.10–1.01 g, from Zha Lin, Yu Lin Gu and Nai Sa-Bainang) show various uneven blue-green or red zones. Surface-reaching fractures are surrounded by narrow colorless areas. (a) and (b) the samples from Zha Lin mine, (c), (d) and (e) from Yu Lin Gu alluvial fan, (f) from Nai Sa-Bainang mine. The photo of (b, c, d, e) at the left is under transmittance light, and right is under diffused transmittance light. Photomicrographs by A. Abduriyim; magnified 10x.

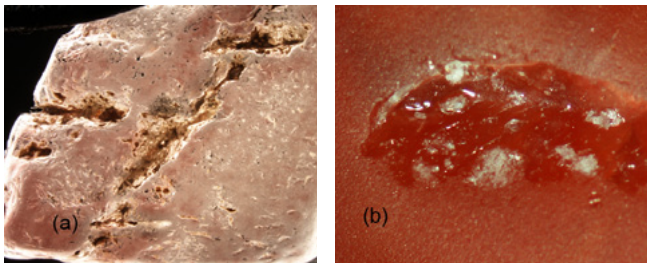

Figure 5. (a), some of the Tibetan samples from three localities have a smooth water-worn appearance but with chemical etching pits, cavities and channels. (b), colorless or white viscous glassy residue can be seen on the surface. Photomicrographs by A. Abduriyim; magnified 12x and 20x.

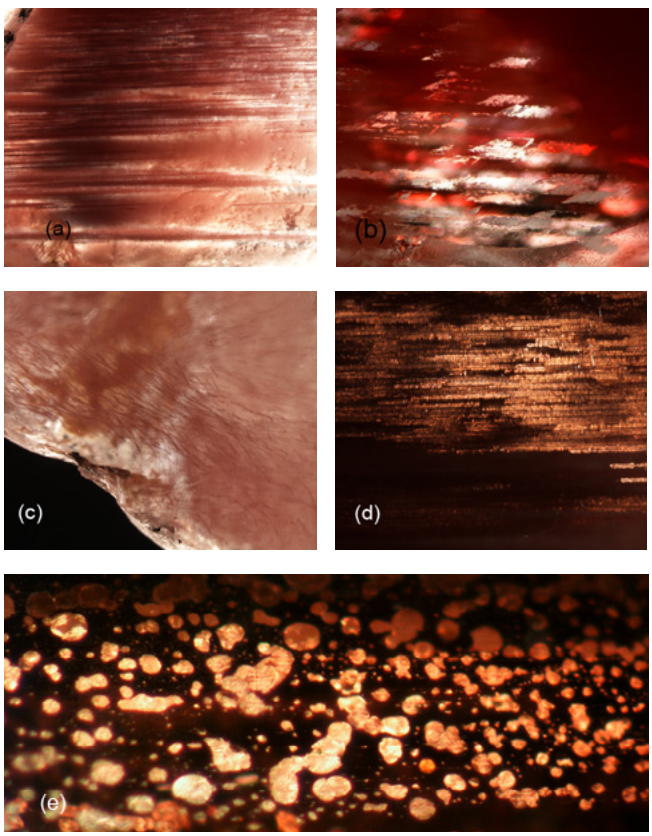

Figure 6. Some internal features noted in the Tibetan andesine included plenty of twin lamellae which are parallel to [010] (a), hollow channels (b), irregular dislocations and turbid milky clouds (c), and rare schiller from the presence of native copper inclusions (d). Copper platelets are well known in Oregon labradorite, but those platelets tend to be much larger than Tibetan samples (e). Photomicrographs by A. Abduriyim; magnified 15–25x.

weak red-green pleochroic stone appeared red in white incident light. Examination with a gemological microscope revealed that most of the Zha Lin and Yu Lin Gu samples contained prominent twin lamellae that were parallel to the {010}, parallel lath-like hollow channels, and pipe-like tubes (figure 6a and b). They also contained irregular dislocations

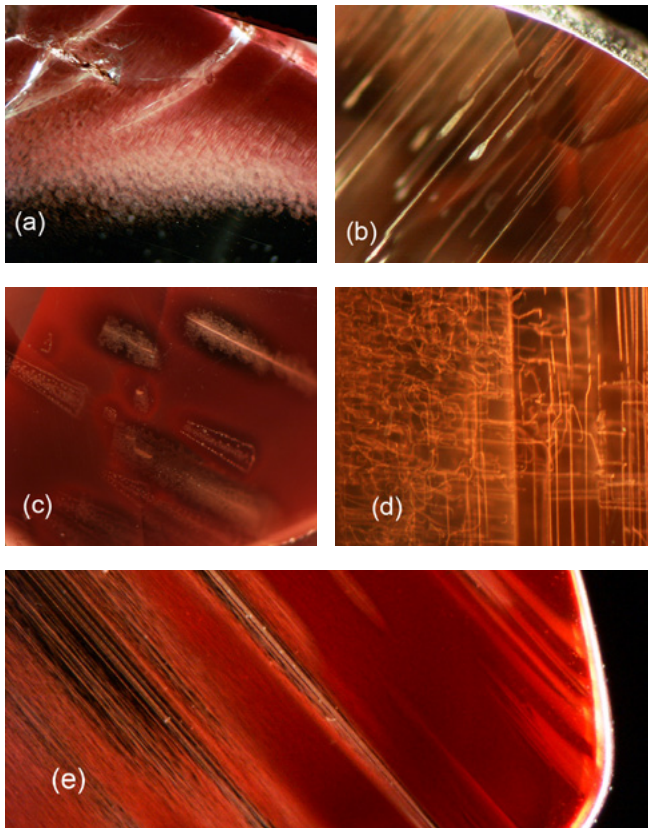

Figure 7. The known-treated samples from Xi'an and Shen Zhen showed numerous pipes (a), tube-like structures and discoid fractures (b), a recrystallized white residue filling the lath-like hollow channels (c), dislocations (d) and cloud-like inclusions (e). Photomicrographs by A. Abduriyim; magnified 20–25x.

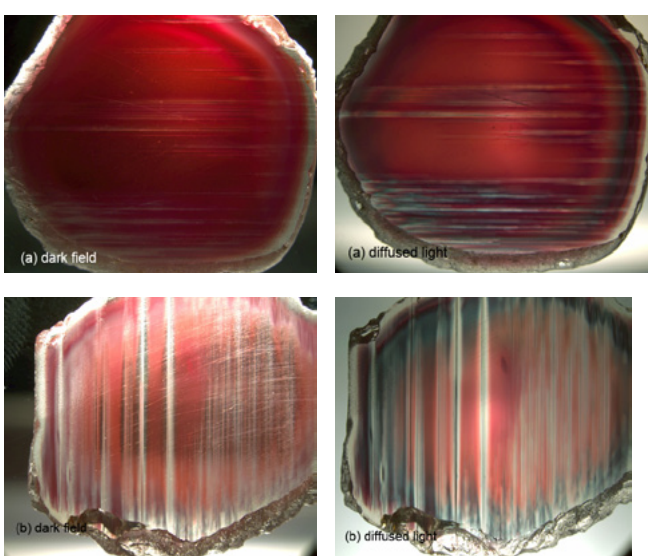

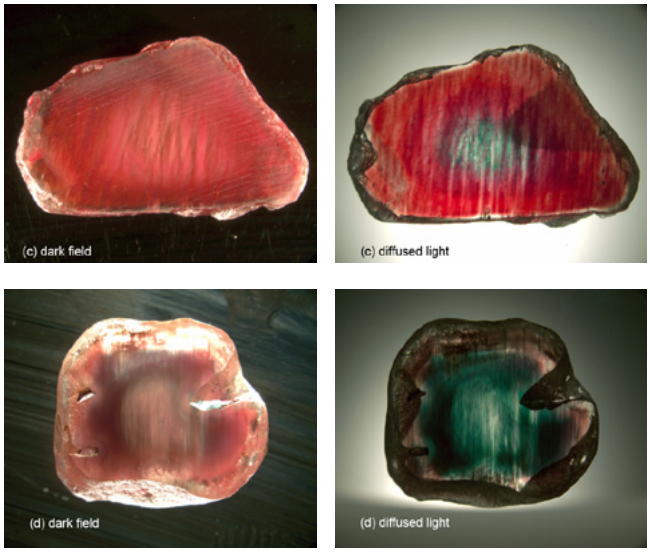

Figure 8. These layer-by-layer concentric color zones appeared in the known-treated andesine. Such features are more distinct than in the Tibetan samples examined and may be indicative of the treatment process. (a) and (b) the samples from Xi'an, (c) and (d) from Shen Zhen, China. The photo of (a, b, c, d) at the left is under transmittance light, and right is under diffused transmittance light. Photomicrographs by A. Abduriyim; magnified 10x.

and color patches caused by milky turbidity from fine granular inclusions (figure 6c). A few stones also displayed healing fractures with no difference of light reflection on the surface. Some contained native copper grains or platelets, which produced reddish orange schiller after polishing (figure 6d). Similar copper platelets are known in Oregon labradorite, but those platelets tend to be much larger (figure 6e). None were seen in the known-treated samples from this study.

The known-treated samples contained pipe and tube-like structures, discoid fractures, a recrystallized white residue filling the lath-like hollow channels, dislocations, and cloud-like inclusions (figure 7). Overall, these resembled the internal features seen in the Tibetan andesine. Distinct concentric color fluctuations from the rim to the core were present in some of the known-treated stones, however (e.g., figure 8). These layer-by-layer color zones appeared more distinct than in the Tibetan samples.

Surface Residue Features

Microscopic observation of the samples from all three reported Tibetan localities revealed surface residues in

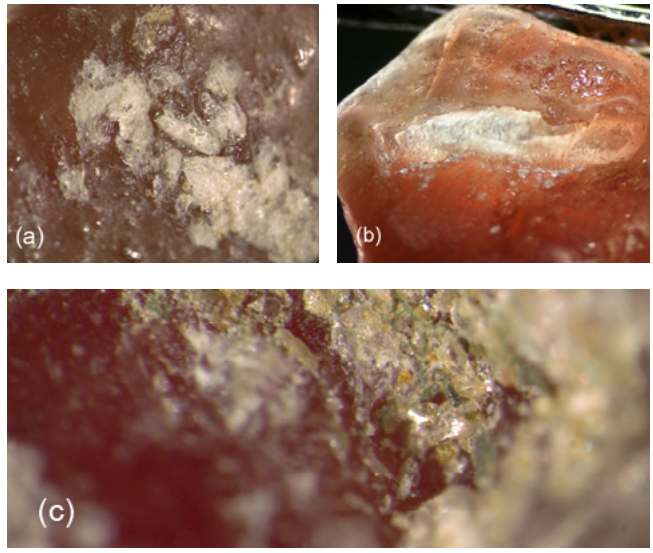

Figure 9. Colorless/white, yellow surface residues can be observed on the surface, fractures and chemical etched cavities of the samples from all three reported Tibetan localities (a, b, c). Photomicrographs by A. Abduriyim; magnified 15-25x.

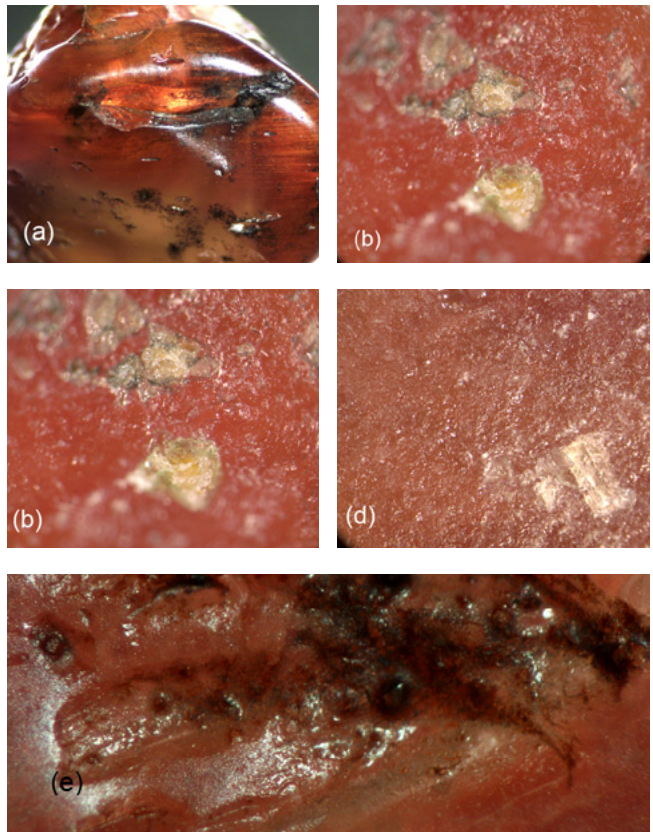

Figure 10. Microscopic observation of known-treated andesine samples revealed the characteristic surface residues such as viscous glassy flux materials on the surface. All pits, fractures and cavities were covered by black residue (a),. Colorless/white, yellow and black-green melted glassy residues overlap the whole surface of the samples and in chemical etched cavities, (b, c, d),. Gas bubble-like residues strongly indicate an artificial treatment process (e). Photomicrographs by A. Abduriyim; magnified 12-25x.

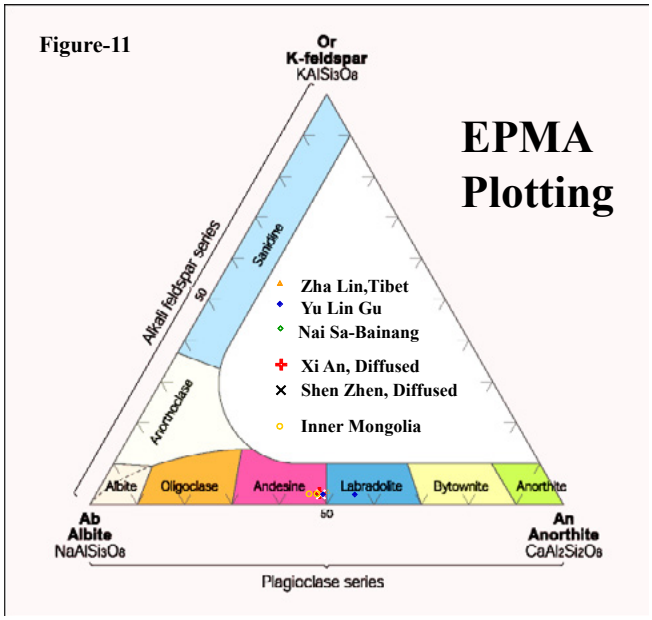

Figure 11. Composition of Tibetan red andesine from three localities, copper-diffused known treated red andesine from Xi'an and Shen Zhen, and Inner Mongolian pale yellow andesine were plotted in a ternary diagram of three end members orthoclase (Or), albite (Ab) and anorthite (An). EPMA data of two samples from Zha Lin are signed as an orange color triangle, Yu Lin Gu samples are in blue rhombic, Nai Sa-Bainang are in green, copper diffused samples from Xi'an are indicated by red plus sign and Shen Zhen samples are in black cross, and yellow circle for Inner Mongolian materials. Except for one sample from Yu Lin Gu placed in the labradorite field, these are near the border of andesine with labradorite.

the fractures, cavities, and depressions of many specimens (figure 9). The residues ranged from transparent to translucent and were colorless/white, yellow, orange, and black. The colorless/white fragments or glassy residues were identified as crystalline alpha quartz and feldspar by Raman spectroscopy, though some residues did not display clear spectra.

Some known-treated andesines showed very characteristic surface residues such as viscous melted glassy material (colorless or white) and gas bubbles. Plenty of tiny spotty numerous particles covered the full surface of these materials, a highly magnification observation by SEM is need. The factures and cavities were covered by black residue (figure 10). Raman analysis was unable to show any spectra that could be assigned to any crystalline mineral from some white glassy residues on the surface, suggesting that these residues are in amorphous structure.

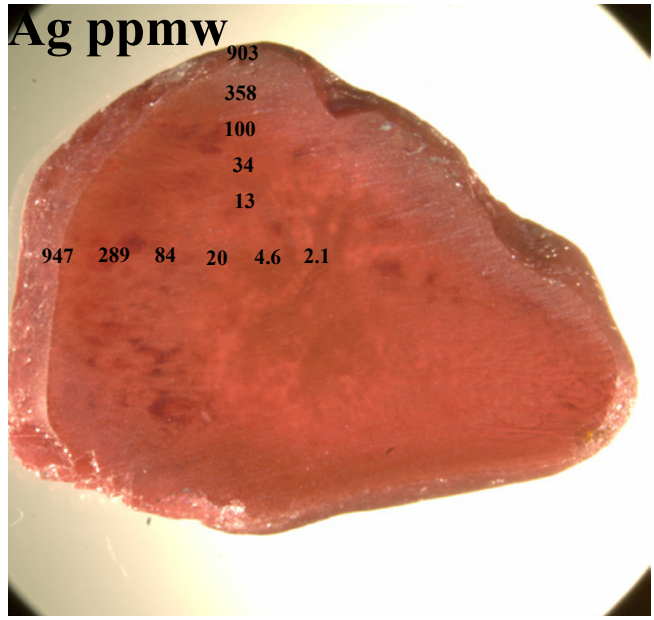

Figure 12. Two compositional traverses analyzed by LA-ICP-MS showing copper and silver from rim to interior of andesine crystal from Yu Lin Gu area. Cu distribution did not show any flexible diminution toward the center of the sample, but Ag appeared to rich at the rim and diminish toward the interior significantly.

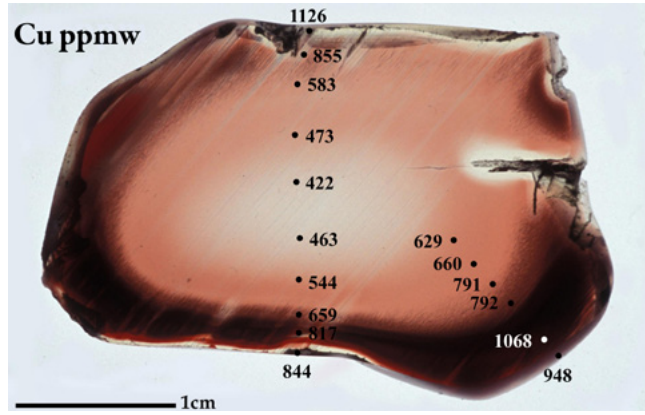

Figure 13. The Cu content in the known treated samples from Xi'An and Shen Zhen appeared to diminish toward the center of the stone.

Chemical Composition

Microprobe analysis of two andesine samples from Zha Lin yielded a composition of Ab_{46-47}:An_{49-50}:$Or_{3.3-3.8}$ (expressed as mol.% albite:anorthite:orthoclase). They plotted in the andesine field, near the border with labradorite (figure 11). One samples from Yu Lin Gu showed a similar range of major elements but with more variable anorthite contents (An_{51}), which placed them at the border of andesine-labradorite

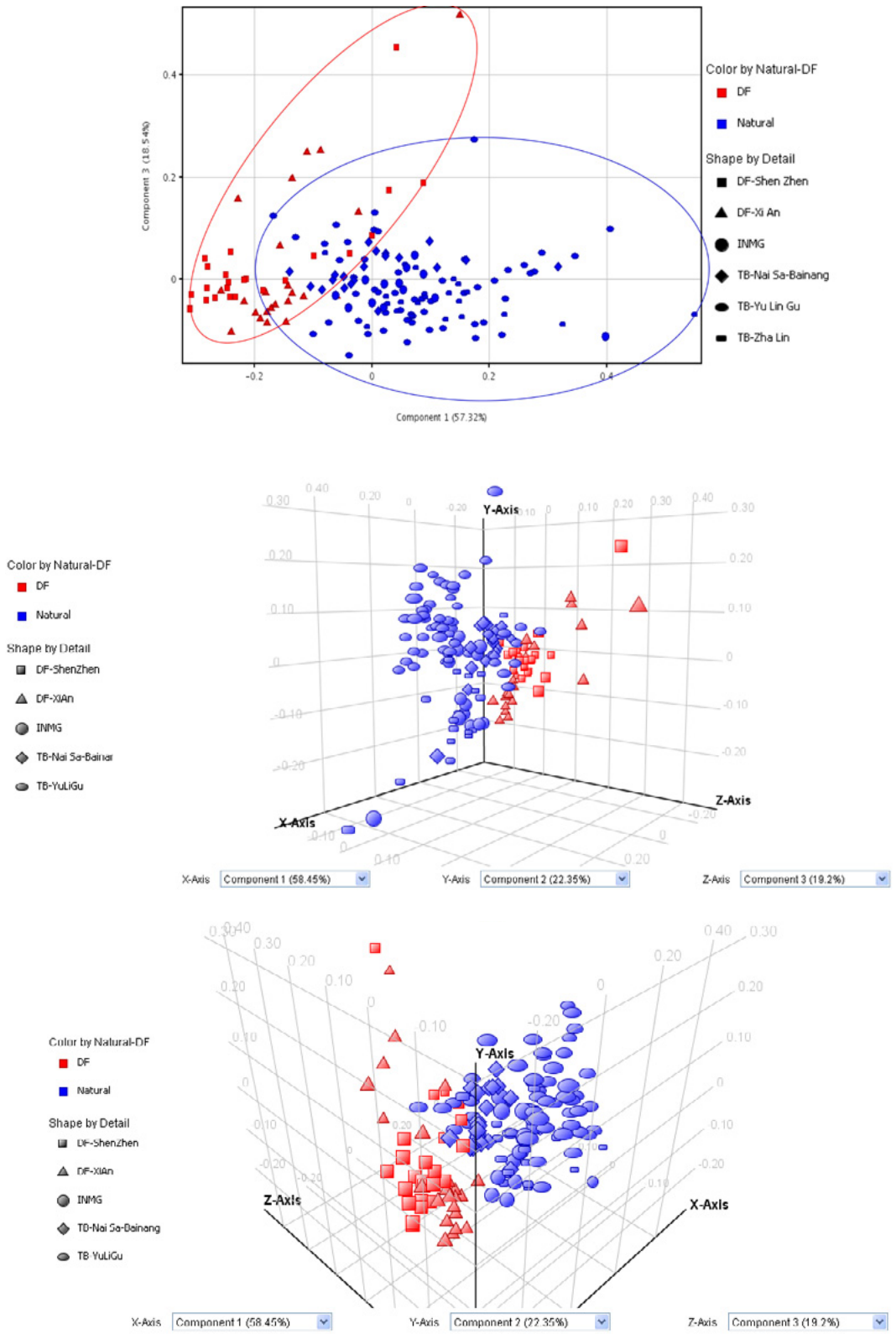

Figure 14. Trace-element data of the Tibetan andesines (blue) and known-treated samples (red) was processed by multivariate statistical analysis into this principal component diagram. Ten isotopes (^{39}K, ^{49}Ti, ^{57}Fe, ^{69}Ga, ^{88}Sr, ^{107}Ag, ^{137}Ba, ^{139}La, ^{140}Ce, and ^{208}Pb) were categorized into two parameters as component 1 and component 3. There is ~30% overlap between the two groups. 3-dimention view by plotting with 3 components in different angles. "DF" copper-diffused stone.

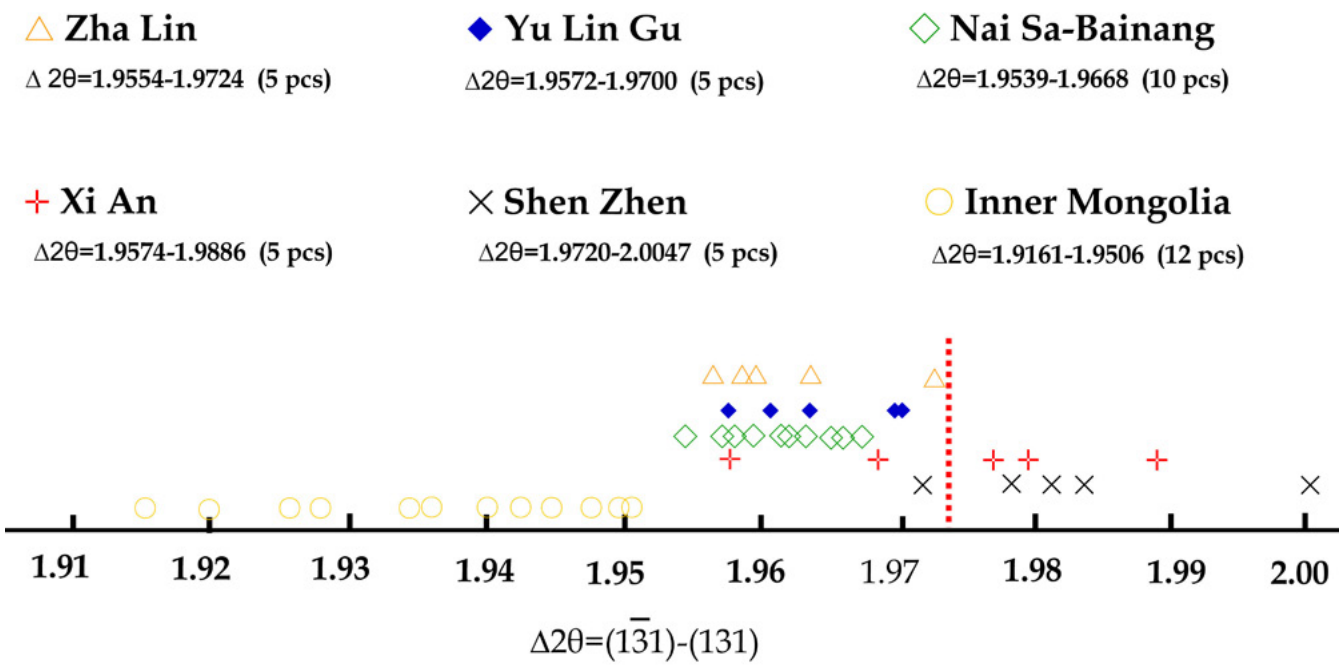

Figure 15. In this diagram, the Δ2ϑ values (calculated using the parameter of $\Delta 2\vartheta = 2\vartheta_{1\bar{3}1} - 2\vartheta_{131}$) obtained from powder X-ray diffraction data show some overlap between Tibetan andesine and known-treated samples. The untreated Inner Mongolian andesine samples have lower Δ2ϑ values.

field. However, five spots were analyzed on another sample (TB-YLG-NP-001) from Yu Lin Gu. The concentration of An mol.% showed very flexible values at 60.17%, 59.03%, 57.74%, 58.34% and 58.02%; some positions may indicate a lamellae growth-zonation feature as solid-solution. Detailed chemical mapping needs to be carried out on the entire sample area (see table 1).

With the exception of the An_{58} sample, these data overlap the compositions given by Rossman (2011) for samples from Tibet and "China." A similar composition was documented in the Nai Sa–Bainang andesine studied by Abduriyim (2009b). Microprobe analyses of four known-treated samples gave compositions of Ab_{46-49}:An_{48-50}:$Or_{2.9-3.3}$, placing them in the andesine field at or near the border with labradorite, indistinguishable from the Tibetan samples. The Zha Lin and Yu Lin Gu andesine contained overlapping copper contents (0.04–0.15 wt.% CuO), similar to the range in the known-treated samples (0.07–0.11 wt.% CuO).

LA-ICP-MS analyses of samples from all three Tibetan localities showed a similar range of Li, B, Mg, P, K, Sc, Ti, V, Mn, Fe, Co, Ni, Cu, Zn, Ga, Ge, Rb, Sr, Y, Zr, Ba, and Pb, as well as the rare-earth elements La, Ce, Pr, Nd, and Eu (see table 2). Except for the trace element of silver, the andesine samples collected from Zha Lin, Yu Lin Gu, and Nai Sa–Bainang were generally indistinguishable from one another. Copper ranged from 270 to 1200 ppmw and tended to be higher in stones with a redder color. Li contents showed corresponding increases with Cu, while Ni concentrations were higher at the surface than in the interior.

Traces of Ag were recorded only in samples from Yu Lin Gu, ranging from 35 to 2900 ppmw. The concentration of Ag at the outer edge of the samples, where a colorless rim was visible, was much higher than the average inside the stones. Also, the amount of Ag appeared to diminish toward the center. In contrast, the distribution of Cu and other trace elements throughout the samples did not show any specific trends (figure 12). Some stones from Zha Lin showed a very low amount of Ag at the surface (~0.12–0.26 ppm by weight) but none in their interior. Ag was not detected in any of the Nai Sa–Bainang stones or in any known-treated or Inner Mongolian materials.

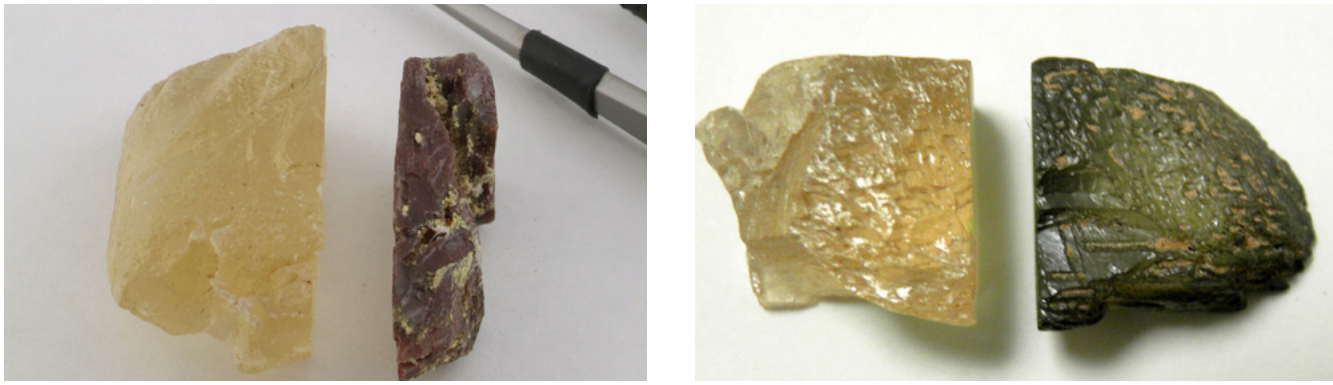

Figure 16. To test whether the Δ2θ parameters were changed by heating, two sets of pale yellow Inner Mongolian samples were selected for copper diffusion experiments. Each sample was cut into two pieces. Left: half of one sample (INMG-DF-001a) was buried in ZrO_2 powder mixed with 2–3% copper powder and diffused at 1160°C for 50 hours, resulting in a red color. Right: the half of the other stone (INMG-DF-002a) was packed into Al_2O_3 powder mixed with 2–3% copper powder and heated at 1050°C for 24 hours, which caused it to turn green. The remaining halves were retained as control samples.

The known-treated samples showed trace-element contents similar to those of the Tibetan stones, but the Cu content decreased from the rim toward the core in most of them (figure 13). Barium contents were slightly lower (99–142 ppmw) than in the Tibetan andesine (123–166 ppmw)

Multivariate statistical analysis of the trace-element data yielded the principal component diagram shown in figure 14. Ten isotopes (^{39}K, ^{49}Ti, ^{57}Fe, ^{69}Ga, ^{88}Sr, ^{107}Ag, ^{137}Ba, ^{139}La, ^{140}Ce, and ^{208}Pb) were categorized into two parameters as component 1 and component 3, and data were plotted into this principal component diagram. The blue symbols represent the 80 samples from the three reported Tibetan localities and the 12 pale yellow samples from Inner Mongolia. The red symbols indicate the 43 known-treated samples. Although there was ~30% overlap between the two groups, the known-treated samples tended to have lower values for the component 3 parameter (<0.2) and relatively high values for the component 1 parameter (up to 0.53).

Powder X-ray Diffraction

Using the parameter of $\Delta 2\theta = 2\theta_{1\bar{3}1} - 2\theta_{131}$, combined with anorthite content, we can determine the Al/Si distribution among the four tetrahedral sites in the plagioclase structure (Ribbe, 1972). The diffraction data for five Zha Lin andesines gave values of Δ2θ = 1.9554°–1.9724°, while five samples from Yu Lin Gu yielded Δ2θ = 1.9572°–1.9700° and 10 from Nai Sa–Bainang were calculated as Δ2θ = 1.9539°–1.9668° (figure 15). Of the known-treated samples, five from Xi'an were in the range Δ2θ = 1.9574°–1.9886° and five from Shenzhen gave Δ2θ = 1.9720°–2.0047°. The copper-diffused samples' tendency to have a higher parameter is reflected by the degree of Al/Si disorder at the tetrahedral site. The temperature at which this disorder formed is probably higher than 800–900°C. The 12 pale yellow samples of Inner Mongolian andesine showed a significantly lower parameter of Δ2θ = 1.9161°–1.9506° compared to the Tibetan and known-treated samples.

Our copper diffusion experiments confirmed that the Δ2θ parameter can be altered significantly by high-temperature heating. Both diffused samples showed red and green colors (figure 16a and b), and the parameters changed from Δ2θ = 1.9264° to 1.9764° and from Δ2θ = 1.9506° to 1.9811°. The high temperatures associated with laboratory diffusion of Cu into plagioclase are reflected in the increased disorder measured by powder X-ray diffraction. Nevertheless, the cooling history of the reputed Tibetan andesine is unknown, so it is difficult to interpret how the order/disorder data relate to the possibility of laboratory treatment.

CONCLUSIONS

Most of the samples obtained in Zha Lin and Yu Lin Gu during the 2010 expedition were rounded pebbles of lower quality than the attractive gems represented as Tibetan in

Locality Sample number	Zha Lin TB-ZL-OR006-007	Yu Lin Gu TB-YLG-OR001-002	Nai Sa-Bainang* TB-CH-OR001-004	Xi'an XA-DT-R001-002	Shen Zhen SZ-DT-R001-002	Inner Mongolia* INMG-CH-PY001-010
	Oxide (wt.%)	Oxide (wt.%)	Oxide (wt.%)	Oxide (wt.%)	Oxide (wt.%)	Oxide (wt.%)
Na2O	5.00-5.06	3.79-5.17	5.29-5.52	5.52-5.31	5.52-5.66	5.56-5.70
Al2O3	27.9-27.46	28.61-29.17	27.55-27.75	29.41-29.2	28.92-28.99	27.32-27.55
SiO2	55.82-56.36	56.08-54.44	55.80-55.99	53.63-54.0	54.37-54.06	55.9-56.2
K2O	0.57-0.63	0.54-0.54	0.53-0.56	0.54-0.56	0.52	0.52-0.56
CaO	9.94-9.59	10.13-9.93	9.84-10.18	10.18-9.99	10.26-10.06	9.66-10.0
FeO	0.36-0.40	0.4-0.38	0.29-0.34	0.36-0.39	0.35-0.37	0.31-0.35
CuO	0.09-0.15	0.15-0.04	0.05-0.11	0.09-0.08	0.11-0.07	bdl
SrO	0.11-0.12	0.11-0.11	0.10-0.13	0.11-0.1	0.1	0.06-0.14
MgO	0.07	0.07-0.08	0.06-0.07	0.08-0.09	0.08-0.07	0.07
TiO	0.07-0.09	0.07	0.06-0.07	0.07	0.06	0.06-0.07
BaO	0.05-0.04	0.02-0.04	0.02-0.05	0.01-0.008	0.01-0.02	0.01-0.03
AgO	bdl	0.03-0.01	bdl	bdl	bdl	bdl
Total	100	100	100	100	100	100
Atom						
Na	0.44-0.45	0.34-0.45	0.46-0.48	0.48-0.47	0.46-0.50	0.48-0.49
Al	1.48-1.46	1.51-1.55	1.46-1.47	1.57-1.56	1.54-1.55	1.45-1.46
Si	2.52-2.54	2.52-2.45	2.52-2.53	2.43-2.44	2.46-2.45	2.52-2.53
K	0.03	0.03	0.03	0.03	0.03	0.03
Ca	0.48-0.47	0.48	0.48-0.49	0.49-0.48	0.50-0.49	0.46-0.48
Fe	0.01	0.01	0.01	0.01	0.01-0	0.01
Cu	0.01	0.01	0	0-0.01	0	0
Sr	0	0	0	0	0	0
Mg	0	0	0	0	0	0
Ti	0	0	0	0	0	0
Ba	0	0	0	0	0	0
Ag	0	0	0	0	0	0
Total	4.98-4.97	4.90-4.98	4.99-5	5	5-5.02	5
Ab-An-Or composition						
Ab	46.0-47.01	39.47-46.93	46.96-48.73	47.41-46.63	46.63-49	48.61-49.93
An	50.78-49.18	56.9-49.83	48.01-49.94	49.31-50.31	50.31-48.07	46.82-48.31
Or	3.28-3.84	3.59-3.24	3.09-3.26	3.28-3.06	3.05-2.93	3.07-3.23
	Note; Chemical composition data analyzed by EPMA is an average of 5 analyses on per sample, and data shows a value range of					
	numbers sample in each locality. * was studied in Abduriyim 2009a					

Table 1. EPMA chemical composition data of 8 samples from Tibet and China.

Locality	Zha Lin	Yu Lin Gu	Nai Sa-Bainang	Xi'an	Shen Zhen	Inner Mongolia
Sample number	TB-ZL-LA001-020	TB-YLG-LA001-040	TB-BN-LA001-020	XA-DT-LA001-022	SZ-DT-LA001-023	INMG-LA001-012
Major elements (ppmw)						
Na	**35609-54482**	**33378-42187**	**35420-383189**	**34229-42814**	**34451-39412**	**37902-43761**
Al	**147000**	**147000**	**147000**	**147000**	**147000**	**147000**
Si	**243778-301291**	**233295-293976**	**248383-27851**	**233260-290151**	**236606-295269**	**249603-301392**
Ca	**66595-74864**	**65446-74744**	**69306-73404**	**68696-72229**	**68645-71486**	**66916-71010**
Trace elements (ppmw)						
Li	6.4-349	5.8-69	6.5-33	14-30	13-185	6.4-11
Be	bdl	bdl-0.4	bdl	bdl	bdl	bdl
B	bdl-1.8	bdl-2	bdl-1.5	bdl-1.4	bdl-1.6	bdl-0.7
Mg	341-635	414-560	431-646	465-981	428-519	375-520
p	78-109	59-125	80-126	71-130	61-113	66-117
K	3378-7002	3136-4950	3500-4855	3212-4188	3490-4732	3576-5442
Sc	4.5-11.2	1.7-11	3.5-8.7	1.8-5.2	1.7-3.7	2.6-6.5
Ti	381-485	362-426	359-415	364-385	351-397	372-480
V	1.4-2.4	1.3-1.8	1.4-2.2	1.5-2	1.4-2	1.5-2.3
Cr	bdl	bdl-2.1	bdl	bdl	bdl	bdl
Mn	24-42	26-38	29-37	32-53	29-34	28-39
Fe	1329-2636	973-4468	1406-2489	2100-4204	2290-3737	1830-6266
Co	bdl-0.7	bdl-0.8	bdl-0.7	bdl-5	bdl-1.2	bdl-0.8
Ni	bdl-10.5	bdl-14.7	bdl	bdl-9.4	bdl-2.4	bdl-0.6
Cu	411-1153	315-1184	426-852	392-1334	399-2426	bdl-2.3
Zn	2.5-65	2.1-22.7	2.9-7.9	7.6-13	3.5-12	3.1-25
Ga	17-26	17-22	18-24	16-20	17-20	18–26
Ge	bdl-1.2	bdl-1.2	bdl-1.5	bdl-1.4	bdl-1.1	bdl-1.3
Rb	0.7-1.5	0.78-1.1	0.7-1.2	0.7-2.2	0.7-1.1	0.8-1.4
Sr	1025-1219	1044-1251	1079-1172	1038-1111	1025-1116	1070-1150
Y	0.09-0.3	0.1-0.3	0.1-0.2	0.1-0.2	0.1-0.3	bdl-0.2
Zr	bdl-0.6	bdl-0.5	bdl-0.3	bdl-1.7	bdl-0.6	bdl-4.5
Ag	bdl-0.26	35-2889	bdl	bdl-2.6	bdl	bdl
Ba	113-166	126-163	123-158	100-116	99-142	137-167
La	1.2-1.4	1.2-1.7	1.2-1.4	1.1-1.6	1.2-1.7	1.2-1.5
Ce	2.2-2.5	1.9-2.9	2.1-2.9	2.1-2.8	2.1-2.4	2.2-2.8
Pr	0.2-0.3	0.1-0.3	0.1-0.3	0.2-0.3	0.2-0.3	0.2-0.3
Nd	0.7-1.1	0.6-1.2	0.6-1.2	0.6-1.4	0.6-1.2	0.6-1.1
Eu	0.4-0.5	0.2-0.6	0.3-0.5	0.3-0.5	0.3-0.5	0.3-0.5
Pb	0.4-1.3	0.4-1.9	0.4-1.7	0.5-21	0.5-4.5	0.3-1.2
	Note; For LA-ICP-MS; External standard-NIST SRM 610,612, internal standard=28 wt.% Al_2O_3. *ppmw=parts per million by weight, Abbrivi*					
	Data of elements is a value range of minimum to maximum result of analyzed samples, each value is average of three spots on per sample, and					
	Oparation condition; Radio frequency power 1500w, Ablated particle and gas was carried to ICP by He gas.					
	Pulse frequency 5Hz, Laser spot 60μm diameter, laser out power 80% (4.5J/cm²), laser dwell time 120 sec.					

Table 2. LA-ICP-MS analyses of 80 orange-red to red Tibetan samples (20 from Zha Lin and 40 from Yu Lin Gu obtained in 2010, and 20 from Abduriyim's 2008 expedition to Nai Sa–Bainang); 45 known-treated red samples (22 from Xi'an and 23 from Shenzhen), and 12 pale yellow pieces from Inner Mongolia. Results are in ppmw.

the marketplace. The andesine from the Nai Sa–Bainang area generally had a stronger red color, and 4–6% of the production had a high commercial quality.

The gemological properties between the Tibetan and the known-treated samples obtained by the expedition overlapped. Both the Tibetan and the known-treated andesines may host glassy surface residues consisting of colorless or white patches of silica and feldspar. Raman spectra confirmed that most of the silica fragments in Tibetan andesine have a quartz crystalline structure, but some glassy residues of known-treated materials are amorphous silica. Known-treated materials from Xi'an and Shenzhen displayed a viscous -like melted residue on the entire surface and a black residue covering the fractures and cavities. The reddish orange schiller effect due to native copper grains can be seen in a few of the samples from Zha Lin and Yu Lin Gu, but the known-treated materials did not show such a phenomenon.

The chemical properties also overlapped, except for the significant amounts of Ag in the Yu Lin Gu samples and a possible depletion of Ba in the known-treated stones. Multivariate statistical analysis of the chemical data in a principal component diagram gave a 30% overlap in the Tibetan and known-treated stones. Powder X-ray diffraction data showed some overlap between the two, but copper-diffused samples tended to have a higher parameter, which is reflected by the degree of Al/Si disorder at the tetrahedral site.

Argon isotopic studies by Dr. George Rossman indicated that the samples from Zha Lin and Yu Lin Gu (none of which had glassy surface residues) had not been exposed to the high temperatures associated with diffusion treatment (Rossman, 2011).

Our research has shown that to date there is no single analytical technique to separate the natural Tibet material from the treated stones from China. This separation might be made using a combination of several advanced techniques, such as microscopic observation of internal features, LA-ICP-MS chemical analysis, X-ray powder diffraction $\Delta 2\theta$ parameter measurement (or single-crystal X-ray diffraction), and argon isotope analysis, but most of them are expensive, destructive, or not widely available, making them impractical for individual specimens.

The field investigation group in 2008 and 2010 expedition found strong field evidence of a genuine andesine deposit at Nai Sa–Bainang and Zha Lin, but could not confirm the authenticity of the Yu Lin Gu occurrence. No primary andesine-bearing source rocks were found in either area, and a more thorough geologic investigation of the region is still needed.

ACKNOWLEDGMENTS

The authors are grateful to Christina Iu (M.P. Gem Corp., Kofu, Japan) for supporting and organizing the field trip, and to Li Tong and his wife Lou Li Ping (Tibet Andesine, Shenzhen, China) for allowing access and guiding us to the localities. Marco Cheung (Litto Gems, Hong Kong) is thanked for arranging a donation of two parcels of Inner Mongolian andesine reportedly treated in China. Special thanks to the ARC National Key Centre for Geochemical Evolution and Metallogeny of Continents (GEMOC), Macquarie University, Sydney, Australia, for LA-ICP-MS chemical analyses; and to Terry Coldham of the Australian Gemmological Association (GAA) for his cooperation with the copper diffusion heating experiment. Ken Farley at Caltech assisted with the argon isotope measurements. Thanks also to Kousuke Kosuda of the National Institute for Materials Science (NIMS), Tsukuba, Japan, for his help with electron microprobe analyses.

ABOUT THE AUTHORS

Dr. Abduriyim (aabduriy@gia.edu) is a GIA consultant in Tokyo, Japan, and was recently chief research scientist at the Gemmological Association of All Japan – Zenhokyo laboratory in Tokyo. Mr. Ross Pogson is mineralogy collection manager in geosciences of Australian museum in Sydney.

REFERENCES

Abduriyim A. (2008) Gem News International: Visit to andesine mines in Tibet and Inner Mongolia. *Gems & Gemology*, Vol. 44, No. 4, pp. 369–371.

Abduriyim A. (2009a) A mine trip to Tibet and Inner

Mongolia: Gemological study of andesine feldspar. *News from Research,* www.gia.edu/research-resources/news-from-research/andesine-mines-Tibet-Inner-Mongolia.pdf, Sept. 10.

Abduriyim A. (2009b) Characteristics of red andesine from the Himalaya highland, Tibet. *Journal of Gemmology*, Vol. 31, No. 5–8, pp. 283–298.

AbduriyimA., Laurs B.M. (2010) Additional field research on Tibetan andesine. *Gems & Gemology*, Vol. 46, No. 4, pp. 310–311.

Abduriyim A., Laurs B.M., Hughes R.W., Leelawatanasuk T., Isatelle F. (2010) Andesine in Tibet–A second field study. *InColor*, No. 15, Fall–Winter, pp. 62–63.

Hughes R.W. (2010) Hunting Barack Osama in Tibet: In search of the lost andesine mines. www.ruby-sapphire.com/tibet-andesine.htm, Nov. 3.

Leelawatanasuk T. (2010) GIT report: Natural red andesine from Tibet: Real or rumor? www.xz-tys.com/en/shownews.asp?id=401, Nov. 12.

Ribbe P.H. (1972) One-parameter characterization of the average Al/Si distribution in plagioclase feldspars. *Journal of Geophysical Research, Solid Earth*, Vol. 77, No. 29, pp. 5790–5797.

Rossman G.R. (2011) The Chinese red feldspar controversy: Chronology of research through July 2009. *Gems & Gemology*,Vol. 47, No. 1, pp. 16–30.

Van Achterberg E., Ryan C.G., Griffin W.L. (1999) GLITTER: On-line interactive data reduction for the laser ablation ICP-MS microprobe. 9th Annual V. M. Goldschmidt Conference, Cambridge, Massachusetts, August 22–27, www.gemoc.mq.edu.au/Abstracts/Abs1998/vanAchterbergh985.htm.

Note: This report accompanies the following article: Abduriyim A., McClure S.F., Rossman G.R., Leelawatanasuk T., Hughes R.W., Laurs B.M., Lu R., Isatelle F., Scarratt K., Dubinsky E.V., Douthit T.R., Emmett J.L. (2011) Research on gem feldspar from the Shigatse region of Tibet, *Gems & Gemology*, Vol. 47, No. 2, pp. 167–180.